Calhoun
Institutional Archive of the Naval Postgraduate School

Calhoun: The NPS Institutional Archive

DSpace Repository

Theses and Dissertations 1. Thesis and Dissertation Collection, all items

1967

Pneumatic oscillator using a vortex amplifier.

Pichini, Leonard Joseph.

Massachusetts Institute of Technology

http://hdl.handle.net/10945/12851

Downloaded from NPS Archive: Calhoun

DUDLEY
KNOX
LIBRARY

Calhoun is the Naval Postgraduate School's public access digital repository for research materials and institutional publications created by the NPS community. Calhoun is named for Professor of Mathematics Guy K. Calhoun, NPS's first appointed -- and published -- scholarly author.

Dudley Knox Library / Naval Postgraduate School
411 Dyer Road / 1 University Circle
Monterey, California USA 93943

http://www.nps.edu/library

NPS ARCHIVE
1967
PICHINI, L.

PNEUMATIC OSCILLATOR USING A VORTEX AMPLIFIER

by

LEONARD J. PICHINI

Thesis Supervisor:
H. H. Richardson,
Assoc. Prof. of Mechanical Engr.

Submitted: May 19, 1967

Thesis
P4868

PNEUMATIC OSCILLATOR
USING A
VORTEX AMPLIFIER

by

LEONARD JOSEPH PICHINI

B. S., UNITED STATES COAST GUARD ACADEMY
(1962)

SUBMITTED IN PARTIAL FULFILLMENT OF THE REQUIREMENTS FOR
THE DEGREES OF MASTER OF SCIENCE AND NAVAL ENGINEER.

at the

MASSACHUSETTS INSTITUTE OF TECHNOLOGY

June, 1967

Signature of Author . . . .
Department of Naval Architecture and
Marine Engineering, May 19, 1967.

Certified by . . . .
Thesis Supervisor.

Certified by . . . .
Reader for the Department

Accepted by . . . .
Chairman, Departmental Committee
on Graduate Students

f'S ARCHIVE ~~Thesis P4868~~
6-T
CHIN, L.

LIBRARY
NAVAL POSTGRADUATE SCHOOL
MONTEREY, CALIF. 93940

PNEUMATIC OSCILLATOR USING A VORTEX AMPLIFIER

by

LEONARD JOSEPH PICHINI

Submitted to the Department of Naval Architecture and Marine Engineering in partial fulfillment of the requirements for the Master of Science Degree in Mechanical Engineering and the Professional Degree, Naval Engineer.

ABSTRACT

The vortex valve pneumatic oscillator is described. Data obtained for variations of inlet area, bias flow and temperature are presented. The input impedance of the valve is determined experimentally and found to have a region of negative resistance. If the valve is supplied through a capacitance (a volume) the combination produces a limit cycle oscillation where pressure in the volume is a function of time.

Theory predicts the frequency of oscillation to be insensitive to the supply pressure. Analysis of the supply pressure versus frequency data shows the oscillator is nearly pressure insensitive.

Theory predicts the frequency of oscillation to be directly proportional to temperature. The static valve characteristics were found to vary with temperature. Therefore, the temperature sensitivity of the oscillator was predicted from the static valve characteristics. The ratio of predicted temperature sensitivity to actual temperature sensitivity was 3.2 to 1.

Thesis Supervisor: Herbert Heath Richardson
Title: Associate Professor of Mechanical Engineering

ACKNOWLEDGEMENTS

I wish to express my gratitude to Dr. H. H. Richardson for his guidance and leadership.

Acknowledgement is due to the Engineering Projects Laboratory staff, to Mr. Adam C. Bell and Mr. David S. Alles for their many helpful suggestions.

Appreciation to the United States Coast Guard for providing me with this opportunity.

Appreciation to Mrs. Madeline Glynn for the speedy and efficient typing of this manuscript.

Special appreciation to my wife, Jeanne, for her patience and encouragement under trying circumstances.

TABLE OF CONTENTS

Page

CHAPTER I INTRODUCTION AND OBJECTIVES 1

1.1 Introduction 1

1.2 Objective. 1

1.3 The Multiple Inlet Vortex Valve 2

1.4 Scope 6

CHAPTER II APPARATUS 8

2.1 Valve Design 8

2.2 Test Apparatus 12

CHAPTER III EXPERIMENTAL DETERMINATION OF STATIC VALVE CHARACTERISTICS 15

3.1 Experimental Procedure 15

3.2 Data 16

3.3 Analysis for Static Characteristics 22

3.4 Dynamic Behavior, Theoretical 25

CHAPTER IV EXPERIMENTAL RESULTS 29

4.1 Geometric Effects 29

4.2 Pressure Sensitivity 32

4.3 Temperature Sensitivity 32

CHAPTER V CONCLUSIONS AND SUGGESTIONS 37

APPENDIX A HEAT TRANSFER EFFECTS 39

APPENDIX B SLOPE LINE INTEGRATION 43

TABLE OF CONTENTS

Page

REFERENCES 49

LIST OF SYMBOLS

A = area

f = frequency

k = ratio of specific heats (c_p/c_v)

p = pressure

R = gas constant

SCFM = standard cubic feet a minute (70° F, 14.7 psia)

T = temperature

t = time

V = volume

W = mass flow rate

$(\ )_i$ = inlet of valve

$(\ )_o$ = outlet of valve

$(\ )_{in}$ = into volume

$(\ )_1$ = number 1 inlets

$(\ )_2$ = number 2 inlets

B = bulk modulus

ρ = density

LIST OF FIGURES

Page

Fig. 1.0 Schematic of a Multiple Inlet Vortex Valve 3

Fig. 1.1 Typical Impedance Characteristic 4

Fig. 1.2 Schematic of Relaxation Oscillator 7

Fig. 2.0 Detailed Drawing of a Vortex Valve Pneumatic Oscillator 9

Fig. 2.1 Bias Side of Vortex Valve 11

Fig. 2.2 Volume Side of Vortex Valve 11

Fig. 2.3 Experimental Setup 13

Fig. 2.4 Apparatus 14

Fig. 3.1 Static Valve Characteristics 17

Fig. 3.2 " " " 17

Fig. 3.3 " " " 17

Fig. 3.4 " " " 17

Fig. 3.5 " " " 18

Fig. 3.6 " " " 19

Fig. 3.7 " " " 20

Fig. 3.8 " " " 21

Fig. 3.9 Schematic of Relaxation Oscillator 23

Fig. 3.10 Slope-line Integration Technique 27

Fig. 3.11 Predicted Temperature Sensitivity 28

Fig. 4.1 Volume Pressure History 30

Fig. 4.2 Volume Pressure History 31

Fig. 4.3 Pressure Sensitivity 33

Fig. 4.4 Temperature Sensitivity 36

CHAPTER I

INTRODUCTION AND OBJECTIVES

1.1 Introduction

The vortex valve is a pure fluid modulator or amplifier. The operation of the device depends on the dynamic interactions between streams of fluid rather than moving parts. The absence of moving parts and the absence of interface problems make the pneumatic oscillator attractive.

However, the sacrifice made for having no moving mechanical parts is difficulty in designing the geometric shapes analytically. In fact, an analytical procedure for complete design does not exist. Therefore, a great deal of the design is accomplished emperically.

1.2 Objective

The objective of this thesis is to design, construct and test a pneumatic oscillator whose frequency of oscillation is insensitive to supply pressure but sensitive to air temperature. Designing a device which is pressure insensitive eliminates the need for regulation of the supply pressure. A fluidic temperature sensor is highly desirable for temperature sensing in systems operating with oxidizing gases or gases at extremely high temperatures.

An ideal application for such a device would be as a component of a fluidic speed control system for a gas turbine.

The plan of attack was straightforward: design an oscillator that is theoretically pressure insensitive and temperature sensitive, vary one geometric parameter to provide more information for future designs and test the device.

1.3 The Multiple Inlet Vortex Valve

A multiple inlet vortex valve is a cylindrical cavity with two opposing sets of tangential inlets arranged so that with either set flowing alone maximum vortex strength is obtained. Figure 1.0 illustrates this geometry. The clockwise inlets are supplied from a plenum above while the counter-clockwise inlets are supplied from a plenum below. The interesting feature provided by the geometry is its input impedance. Input impedance is defined as the slope of the curve of pressure versus mass flow at the counter-clockwise ports while the clockwise ports are supplied with constant mass flow through a choked orifice. The resulting characteristic is as shown in Figure 1.1 Positive flow is defined as flow into the vortex cavity.

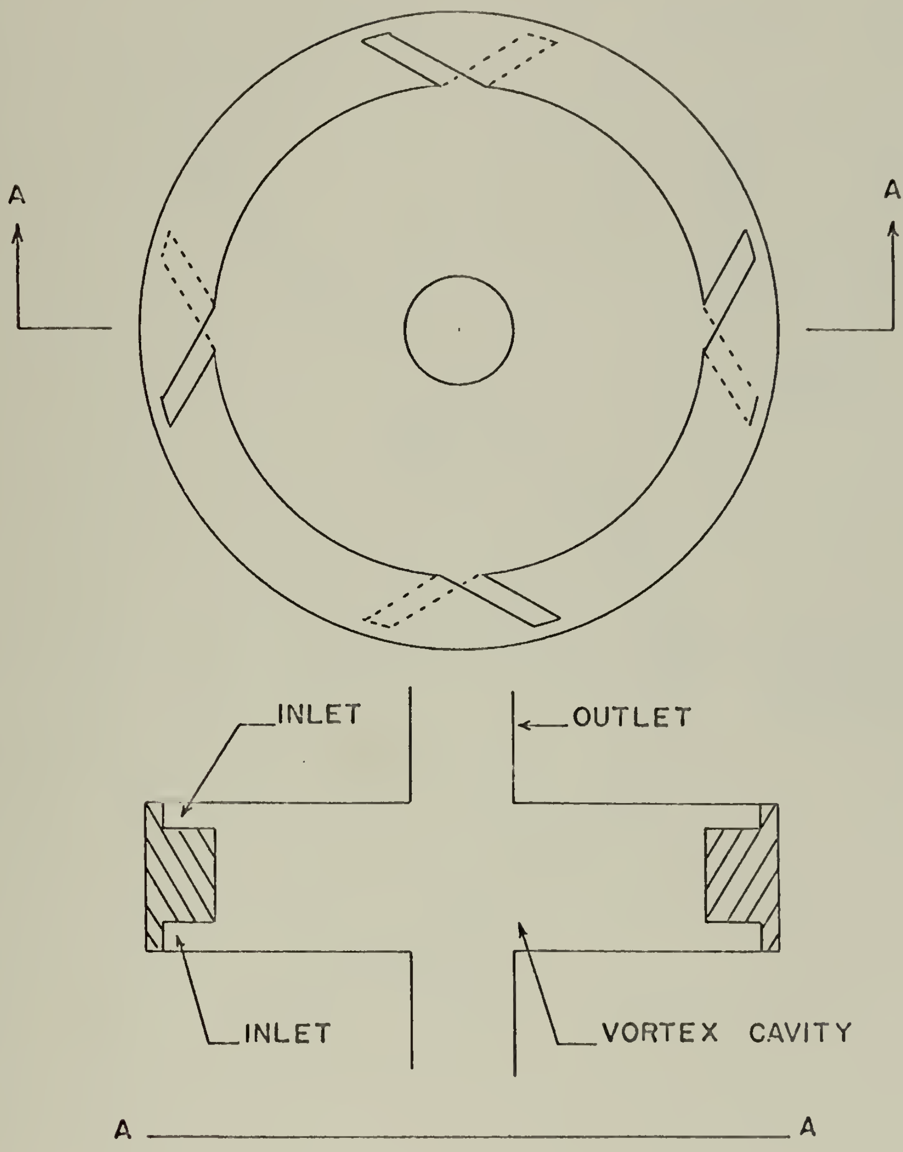

FIGURE 1.0 SCHEMATIC OF A MULTIPLE INLET VORTEX VALVE

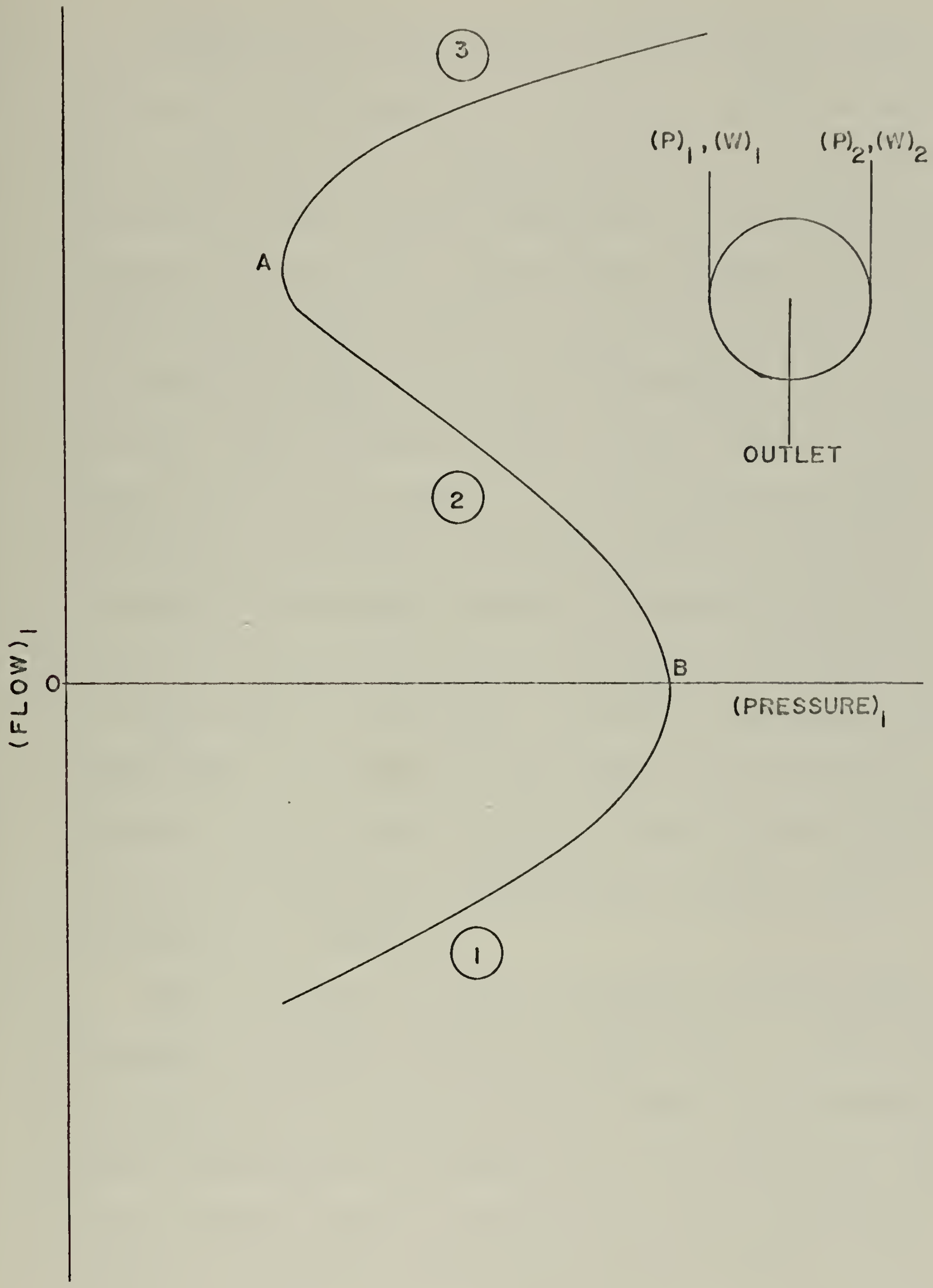

FIGURE 1.1 TYPICAL IMPEDANCE CHARACTERISTIC

A discussion of this characteristic will lead to a better understanding of the operation of the valve. Suppose that the bias flow set of inlets cause a clockwise vortex while flowing alone and therefore the other inlet set would provide a counter-clockwise vortex while flowing alone. For discussion purposes, call the counter-clockwise inlets number 1 and the clockwise inlets number 2. Referring to Figure 1.1, region 1 corresponds to flow out of the vortex cavity through the number 1 inlets. Point "B" corresponds to the pressure caused by the flow through the number 2 inlets with no flow through the number 1 inlets. As flow is introduced into the number 1 inlets, it decreases the vortex strength and causes the pressure to decrease; thus, region 2 of the characteristic is generated. At point "A" the angular momenta of the number 1 and number 2 inlets cancel. As more flow is introduced into the number 1 inlets, a counter-clockwise vortex is formed and the pressure increases; thus, region 3 of the characteristic is generated.

This characteristic provides a negative resistance region and, therefore, a relaxation oscillator could be built. A flow source, a horizontal line on the coordinates of Figure 1.1, would have stable intersections in all regions of the characteristic. However, a pressure source, a vertical line on the coordinates of Figure 1.1, would have stable intersections in regions 1 and 3 and unstable in region 2. Suppose there is a disturbance in the flow

source which causes a flow increase momentarily while the pressure remains fixed, in region 2 the pressure required by the number 1 inlets decreases and, therefore, the source provides more flow until a stable intersection is reached vertically above in region 3.

A relaxation oscillator can be constructed if the number 2 inlets are supplied through a choked valve with a constant bias flow while the number 1 inlets are supplied through a volume. The flow to the volume is set by a choked valve at approximately one-half the bias flow. The volume acts as a pressure source. This combination provides excessive flow for region 1 and insufficient flow for region 3. The result is a limit cycle in which the volume discharges in region 3 until the vortex valve switches to region 1 where the volume charges until the vortex valve switches back to region 3, and the cycle repeats. Figure 1.2 is a schematic diagram of the relaxation oscillator.

1.4 Scope

The scope of this thesis is to design and construct a prototype to examine one parameter of the internal geometry of the valve, to predict and measure the pressure sensitivity of the oscillator, and to predict and measure the temperature sensitivity of the oscillator.

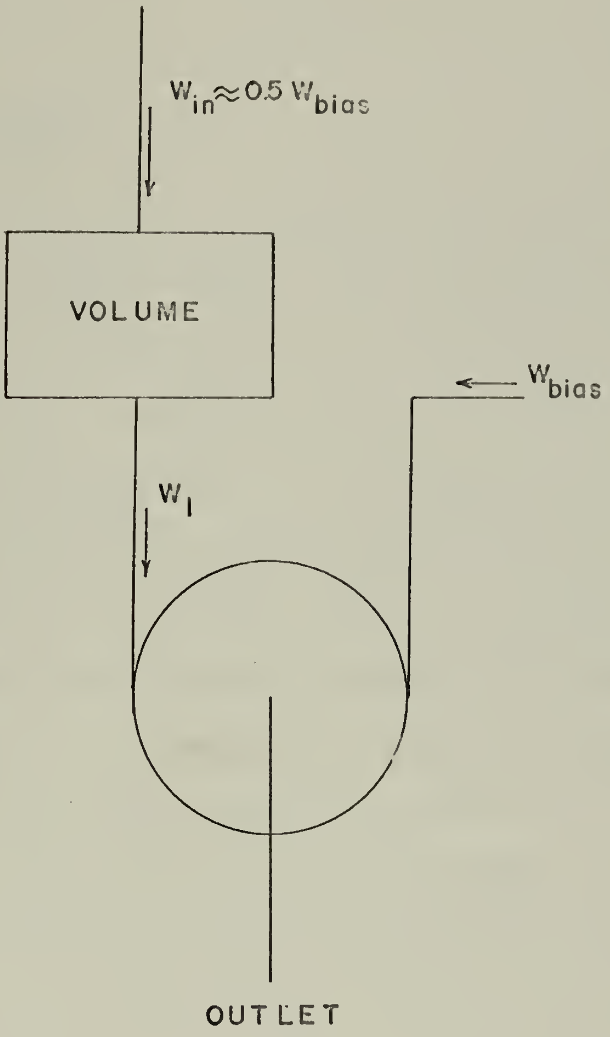

FIGURE 1.2 SCHEMATIC OF RELAXATION OSCILLATOR

CHAPTER II

APPARATUS

2.1 Valve Design

Most of the design has been done empirically due to the absence of analytical methods. The valve has been designed so that the ratio of inlet area to outlet area could be varied. Previous designs, see Reference (1), were constructed so that the opposing tangential inlet sets were lying in the same plane. Therefore, the present design separated the sets of tangential inlets axially by 0.25 inches. Both of the geometric variations will provide useful empirical information for further design and possibly lead to a correlation for analytical design.

The vortex chamber diameter was chosen to be 2.0 inches. The vortex cavity has two outlets; each outlet area is 0.109 sq. inches. To provide versatility in the inlet configuration, twenty-four inlet slots were provided every fifteen degrees around the vortex chamber perimeter. In order to provide twenty-four inlets aroung the circumference of a two inch diameter circle and have part of the circumference remaining, the inlets must make an angle of greater than 35 degrees with a tangent to the circumference of the circle. The 0.125 X 0.125 inch inlets were machined at a 40 degree angle to a tangent at the vortex chamber perimeter. Figure 2.0 is a detailed drawing showing only 4 inlets for clarity.

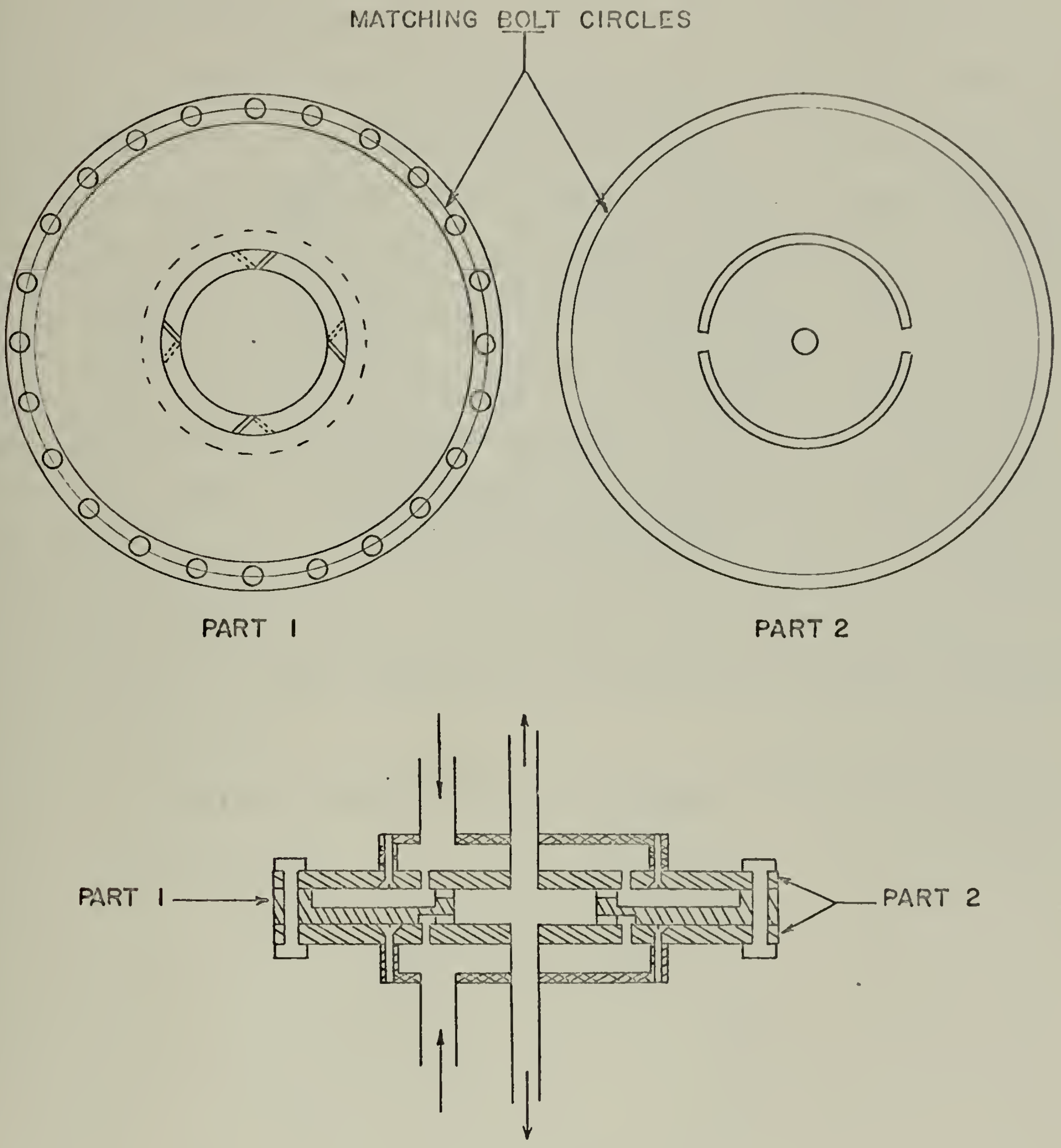

SCALE: 1/20"=1/8"

FIGURE 2.0 DETAILED DRAWING OF A VORTEX VALVE PNEUMATIC OSCILLATOR

The inlets are supplied from plenums above and below part 2.

The volume was designed as an integral part of the valve. This design assured equality of the volume pressure and the pressure at inlets number 1. If the volume is chosen very large compared to the vortex cavity volume, the amplitude of oscillation corresponds closely to the knees of the curve shown in Figure 1.1. The reason for this is that the charging time of the volume is much greater than the switching time of the valve. As the volume approaches the volume of the vortex cavity, the oscillation stops; presumably due to the increasing influence of the valve dynamics. The present device was designed with the volume nearly 4 times larger than the volume of vortex chamber cavity to assure oscillation. The volume = 5.85 cu. in.

Figures 2.1 and 2.2 show a photograph of both sides of part 1 in Figure 2.0.

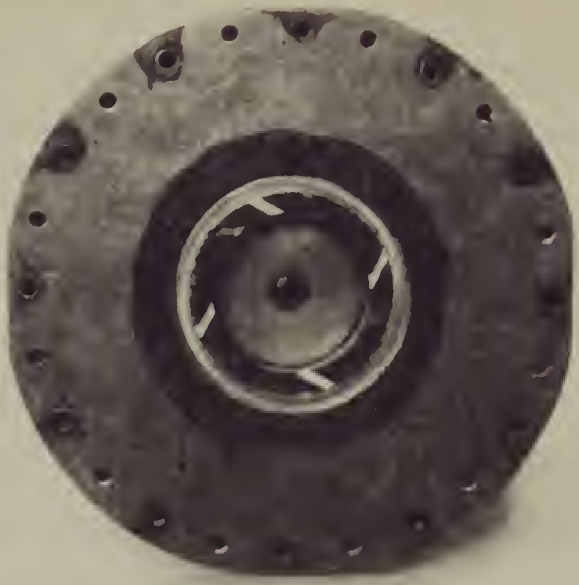

FIGURE 2.1 BIAS SIDE OF VORTEX VALVE

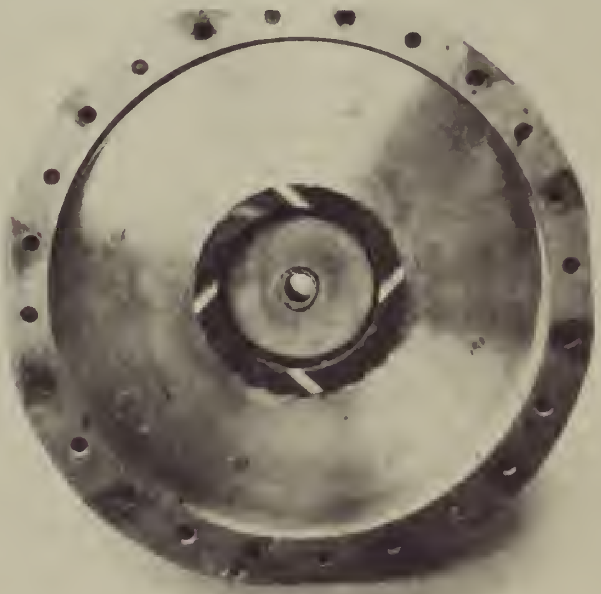

FIGURE 2.2 VOLUME SIDE OF VORTEX VALVE

2.2. Test Apparatus

Figure 2.3 is a schematic of the experimental setup. Figure 2.4 is a photograph of the apparatus. Helicoidal test gages were used to measure pressure and Fischer-Porter variable area meters were used to measure flow rates. The air heater was a 4.5kw Wiegand gas heater. Temperatures were measured with copper-constantan thermocouples. Pressure oscillation was measured using a Dynisco PT 25-25 pressure transducer. Frequency was measured by stopping a Lissajous figure which was generated with the transducer output on the vertical axis and a sine function generator output on the horizontal axis of an oscilloscope. The frequency was counted using a Hewlett-Packard frequency counter.

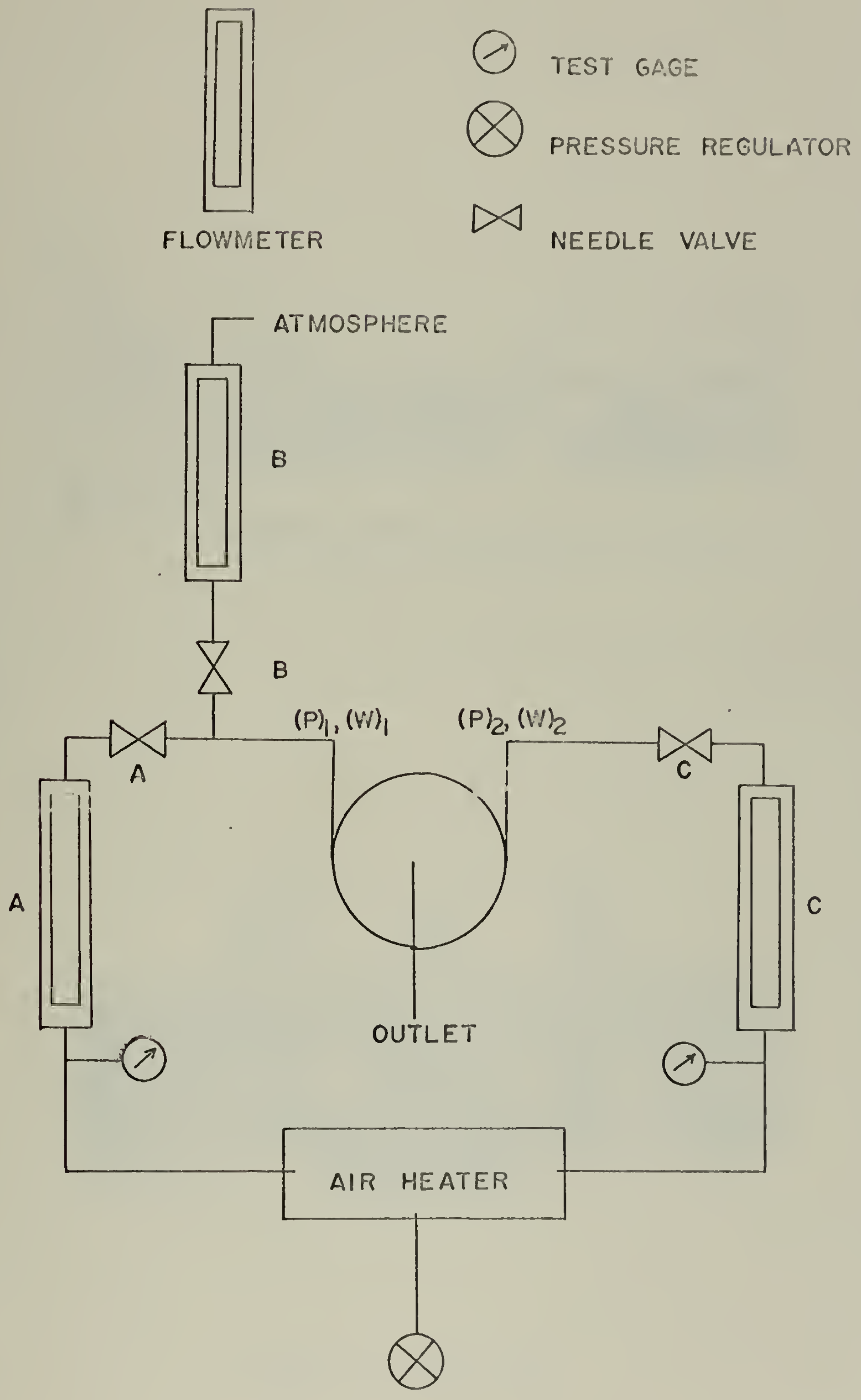

FIGURE 2.3 EXPERIMENTAL SETUP

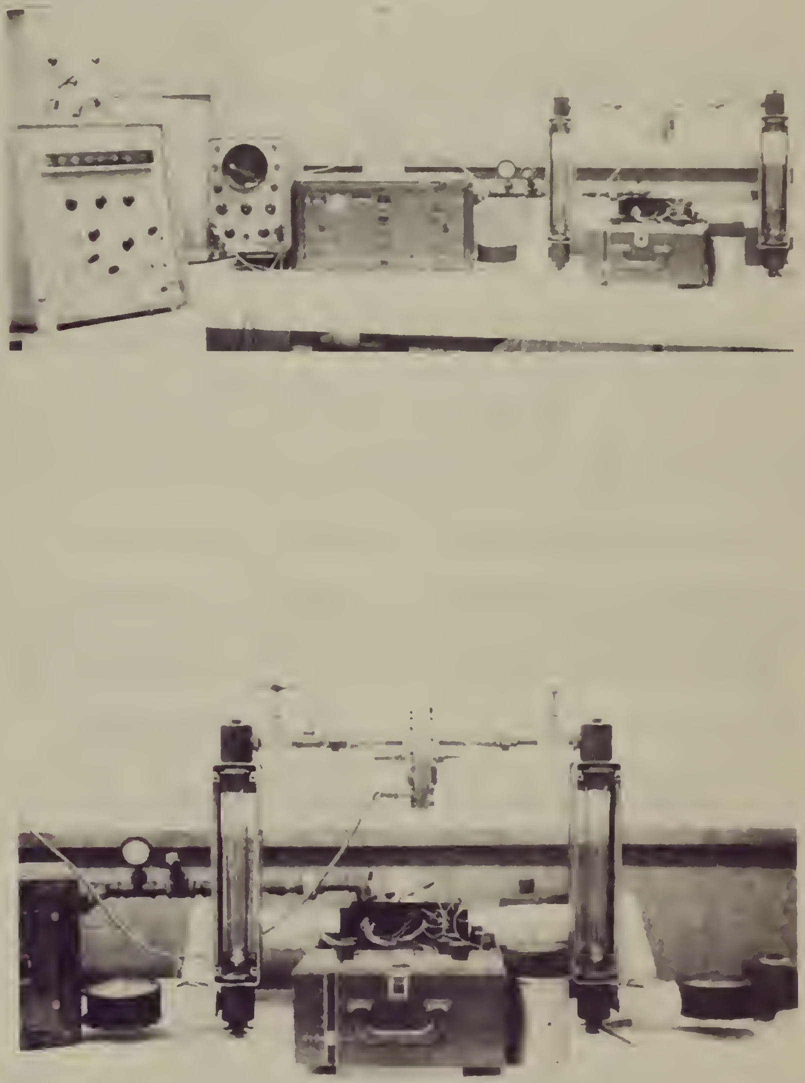

FIGURE 2.4 APPARATUS

CHAPTER III

EXPERIMENTAL DETERMINATION OF STATIC VALVE CHARACTERISTICS

3.1 Experimental Procedure

Referring to Figure 2.3, the static characteristics of the vortex valve were obtained as follows:

a) The flow metering pressure was set and held constant at 40 psig.

b) Bias flow,"C", was set and held constant at either 11.1 SCFM or 5.25 SCFM.

c) Region 1 of the characteristic curve was obtained by opening valve "B" and recording flow at flowmeter "B" while valve "A" remained closed.

d) Regions 2 and 3 of the characteristic curve were obtained by opening valve "A" and recording flow at flowmeter "A" while valve B remained closed.

e) The pressure at the number 1 inlets was measured with a mercury manometer.

The above procedure was repeated for each of the test conditions shown in Table 3.1.

Leakage flow was 1.6% of a total input of 28.25 SCFM.

3.2 Data

Figures 3.1 to 3.8 show the static valve characteristics for the test conditions of Table 3.1.

TABLE 3.1

TEST CONDITIONS

Test No.	A_i/A_o	Bias Flow (SCFM)	Air Temperature (°F)
T 1	0.30	5.25	65
T 2	0.30	5.25	250
T 3	0.45	5.25	65
T 4	0.45	5.25	250
T 5	0.60	5.25	65
T 6	0.60	5.25	250
T 7	0.91	5.25	65
T 8	0.91	5.25	250
T 9	0.30	11.10	65
T10	0.30	11.10	250
T11	0.45	11.10	65
T12	0.45	11.10	250
T13	0.60	11.10	65
T14	0.60	11.10	250
T15	0.91	11.10	65
T16	0.91	11.10	250

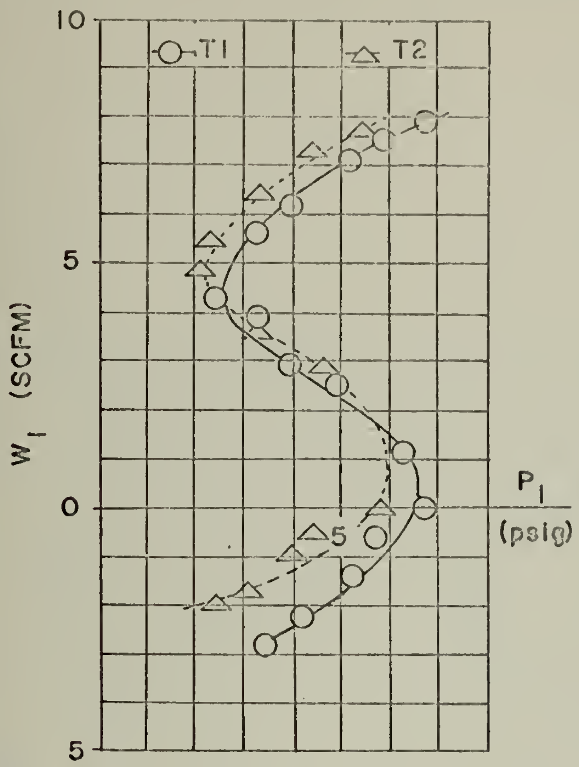

FIGURE 3.1

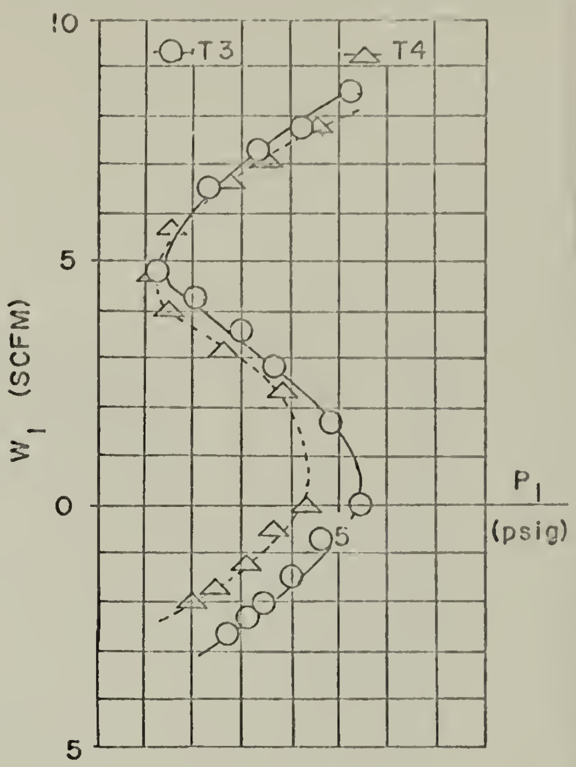

FIGURE 3.2

STATIC VALVE CHARACTERISTICS

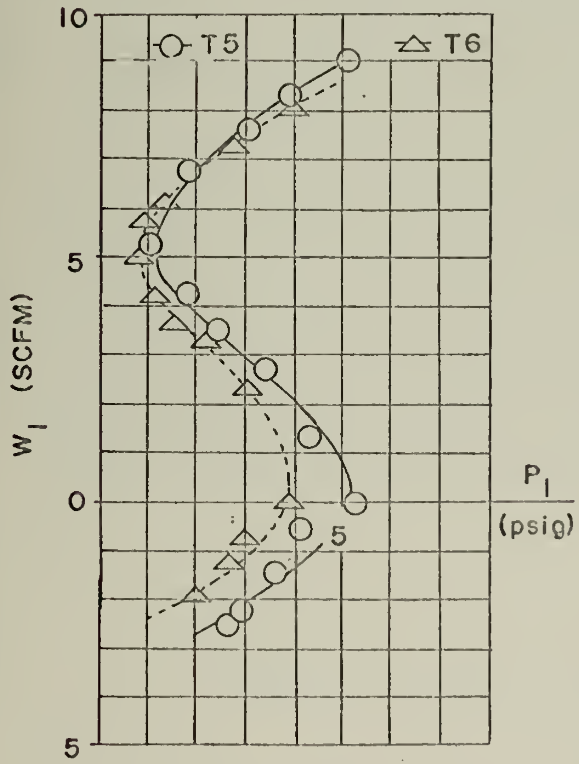

FIGURE 3.3

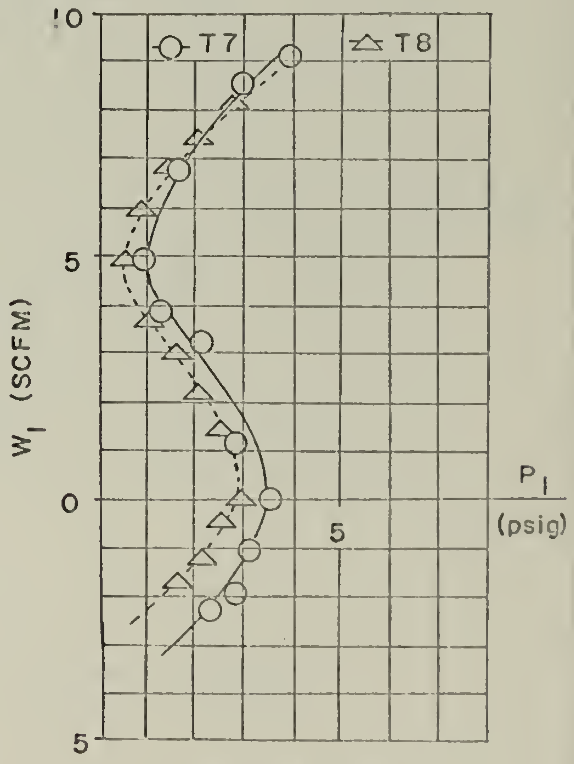

FIGURE 3.4

STATIC VALVE CHARACTERISTICS

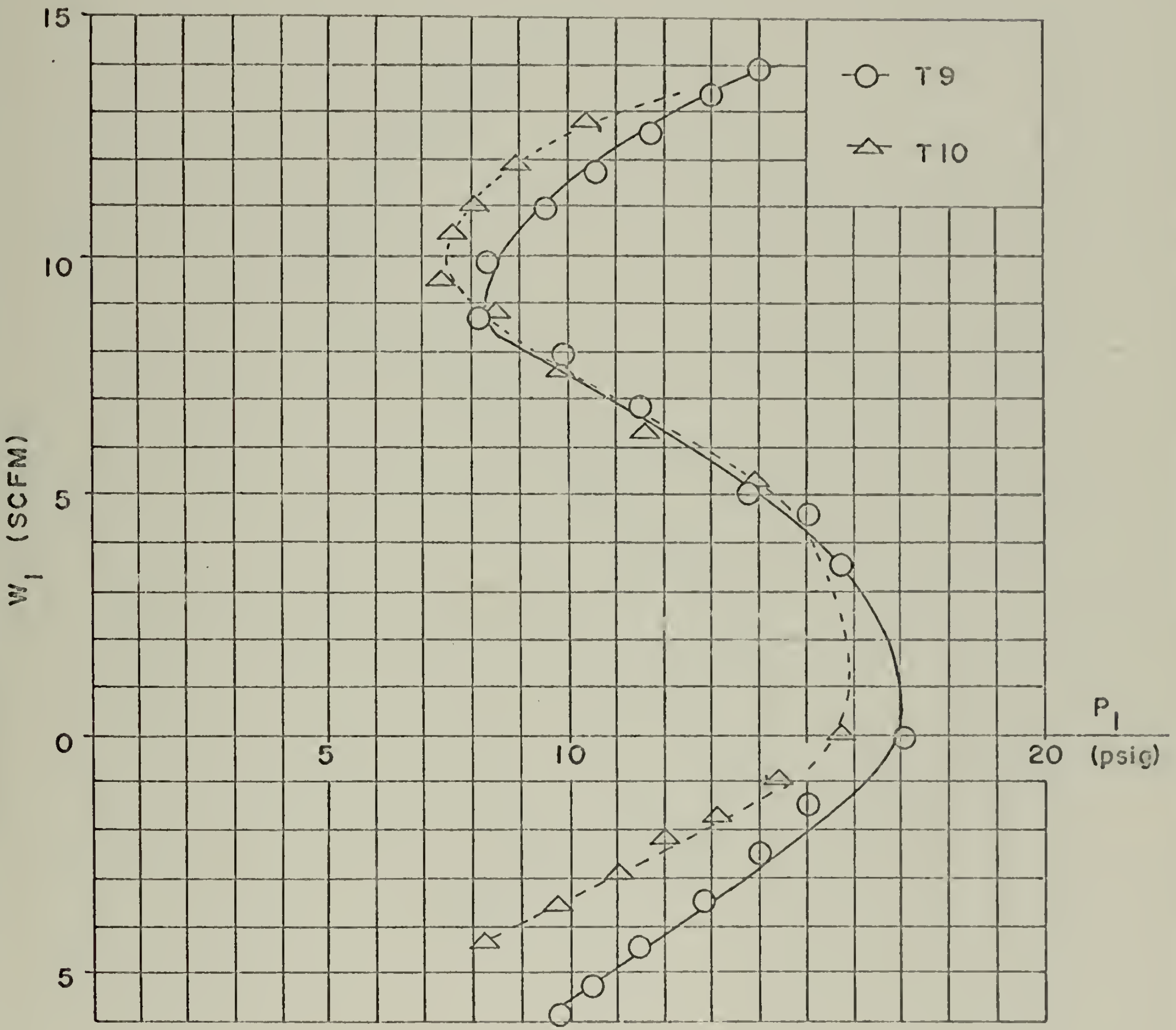

FIGURE 3.5 STATIC VALVE CHARACTERISTICS

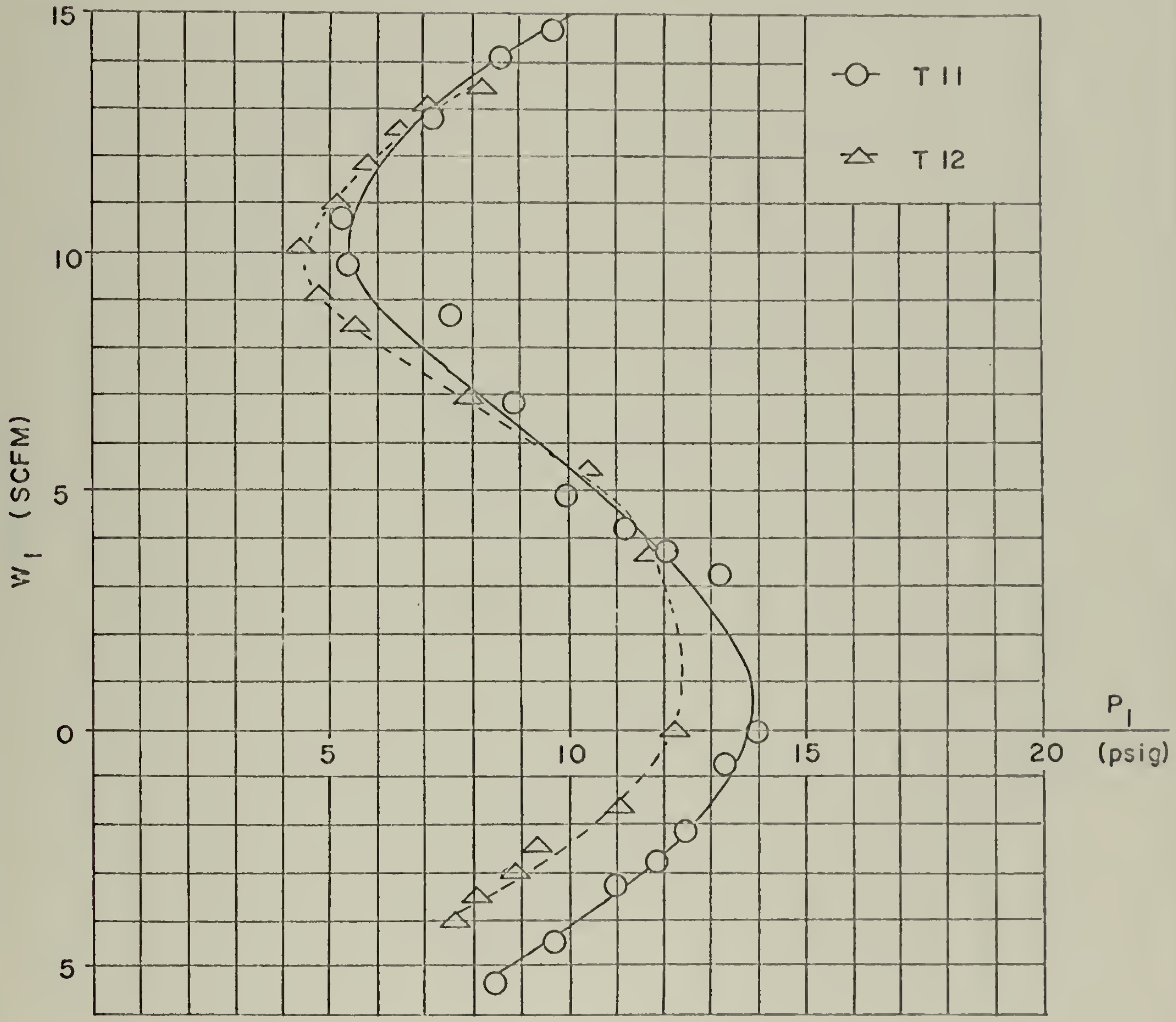

FIGURE 3.6 STATIC VALVE CHARACTERISTICS

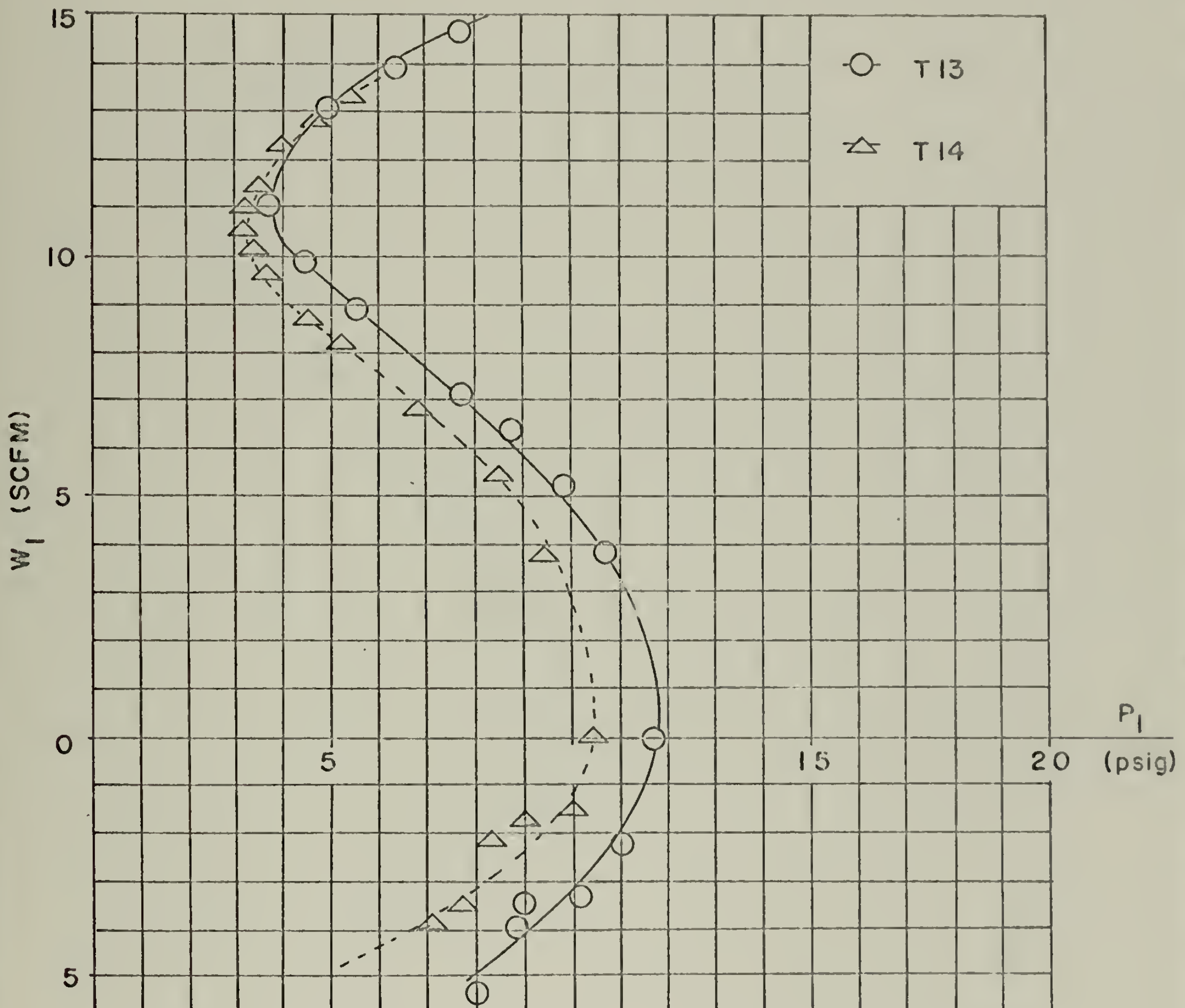

FIGURE 3.7 STATIC VALVE CHARACTERISTICS

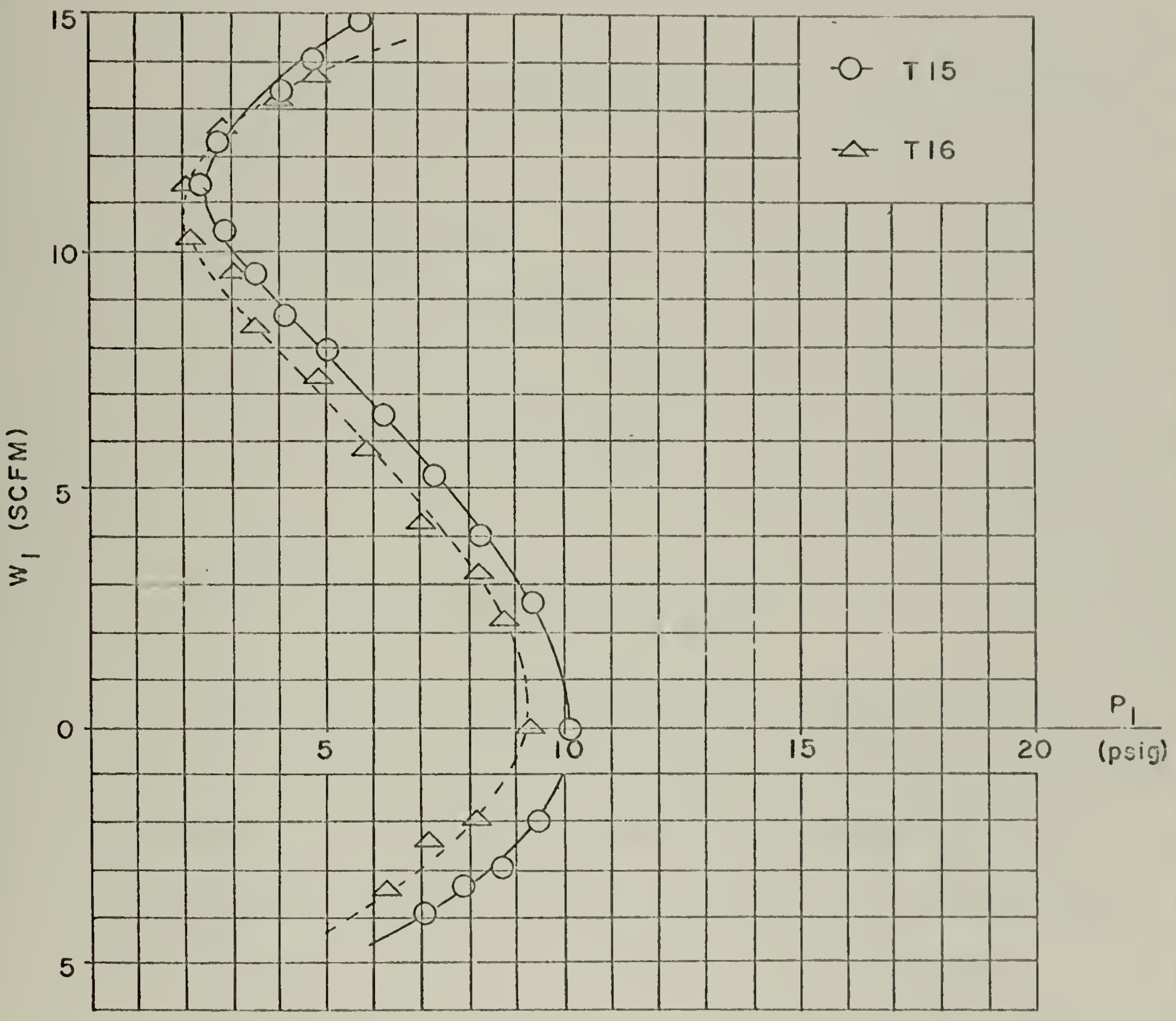

FIGURE 3.8 STATIC VALVE CHARACTERISTICS

3.3 Analysis for Static Characteristics

The analysis for this device was originated by Mr. Adam C. Bell, Reference (1). To provide continuity to this report, it is repeated here.

See Figure 3.9. The governing equations for the device are as follows:

a) Source Equation

$$W_{in} = \text{constant} \tag{1}$$

b) Volume Equation (continuity)

$$W_{in} - W_1 = \frac{\rho V}{B} \frac{dp}{dt} \tag{2}$$

c) Load

$$W_1 = g\,(p_1,\ T,\ \text{geometry}) \tag{3}$$

The volume is an integral part of the valve; therefore, $p_1 = p$. Since W_1 cannot be determined as an analytic function of pressure, p, the equation (2) cannot be integrated directly. Therefore, a graphical technique will be used for the solution. The technique is slope-line integration - see Appendix B.

Rewriting the volume equation in finite difference form:

$$\delta p = (W_{in} - W_1)_{avg.}\ \delta \tau \tag{4}$$

where

$$\delta \tau = \frac{B}{\rho V}\ \delta t \tag{5}$$

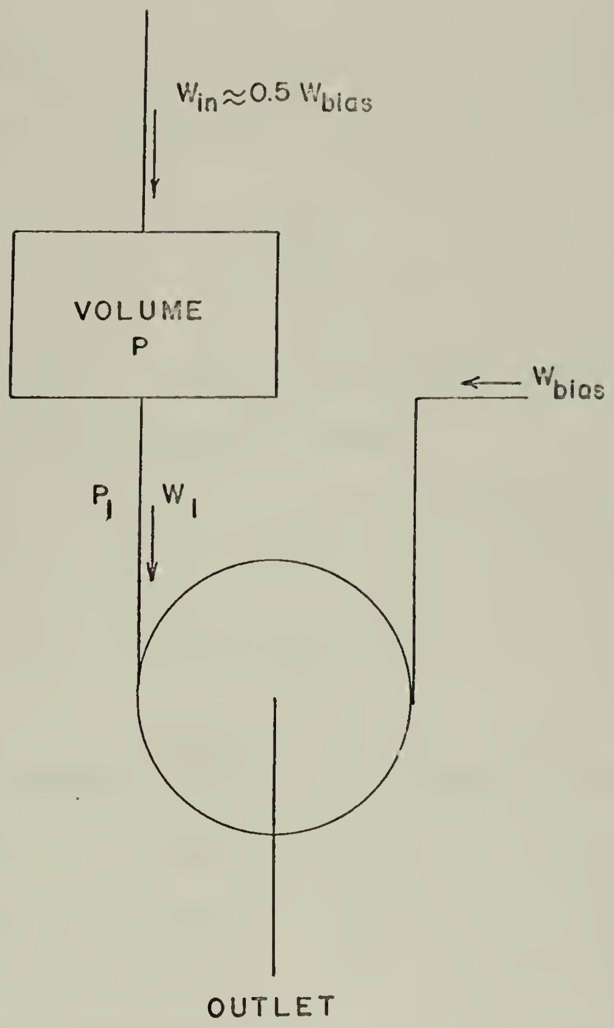

FIGURE 3.9 SCHEMATIC OF RELAXATION OSCILLATOR

This form of the equation states: "the change in pressure over an increment of time is equal to the average net flow into the chamber during that time multiplied by an integrating time factor".

The time constant of the volume is given by:

$$\tau = \frac{\rho V}{B} \tag{6}$$

Frequency of oscillation is inversely proportional to the time constant of the volume. Since

$$B = kp \tag{7}$$

and

$$\frac{\rho}{p} = \frac{1}{RT} \tag{8}$$

the time constant of the volume is inversely proportional to temperature. If the static characteristics were independent of temperature, we could predict that frequency would be directly proportional to temperature. Since the static characteristics do vary with temperature, the temperature sensitivity prediction becomes more involved. Furthermore, the frequency is insensitive to pressure. However, this is only true if mass flows are held constant.

3.4 Dynamic Behavior, Theoretical

The predicted temperature sensitivity was obtained by assuming a linear variation between 65° F and 250° F. The frequency at the end points was predicted using the graphical technique mentioned in Section 3.3 and illustrated in Figure 3.10. Frequency is calculated by relating the $\delta\tau$ period of oscillation to real time through equation (5). Pressure history can also be predicted by plotting pressure versus .

For purposes of illustrating the method, the predicted frequency of oscillation for Figure 3.10 is calculated. Figure 3.10 shows the period of oscillation to be 25 $\delta\tau$. The slope of the lines is:

$$\delta\tau = 2.0 \ \frac{\text{psig}}{\text{SCFM}} \tag{9}$$

Relating this period of oscillation to real time

$$\delta t = \frac{V}{kRT} \ \delta\tau \tag{10}$$

where $V = 3.385 \times 10^{-3}$ cu. ft.

$k = 1.4$

$T = 525\ ^{\circ}R$

$R = 1.72 \times 10^{3}$ ft.^{2}/ sec.^{2} $^{\circ}R$

$\delta t = 49.5$ m sec. therefore

$f = 20.2$ Hz

The results of the integration of the remaining static characteristic curves are shown in Figure 3.11.

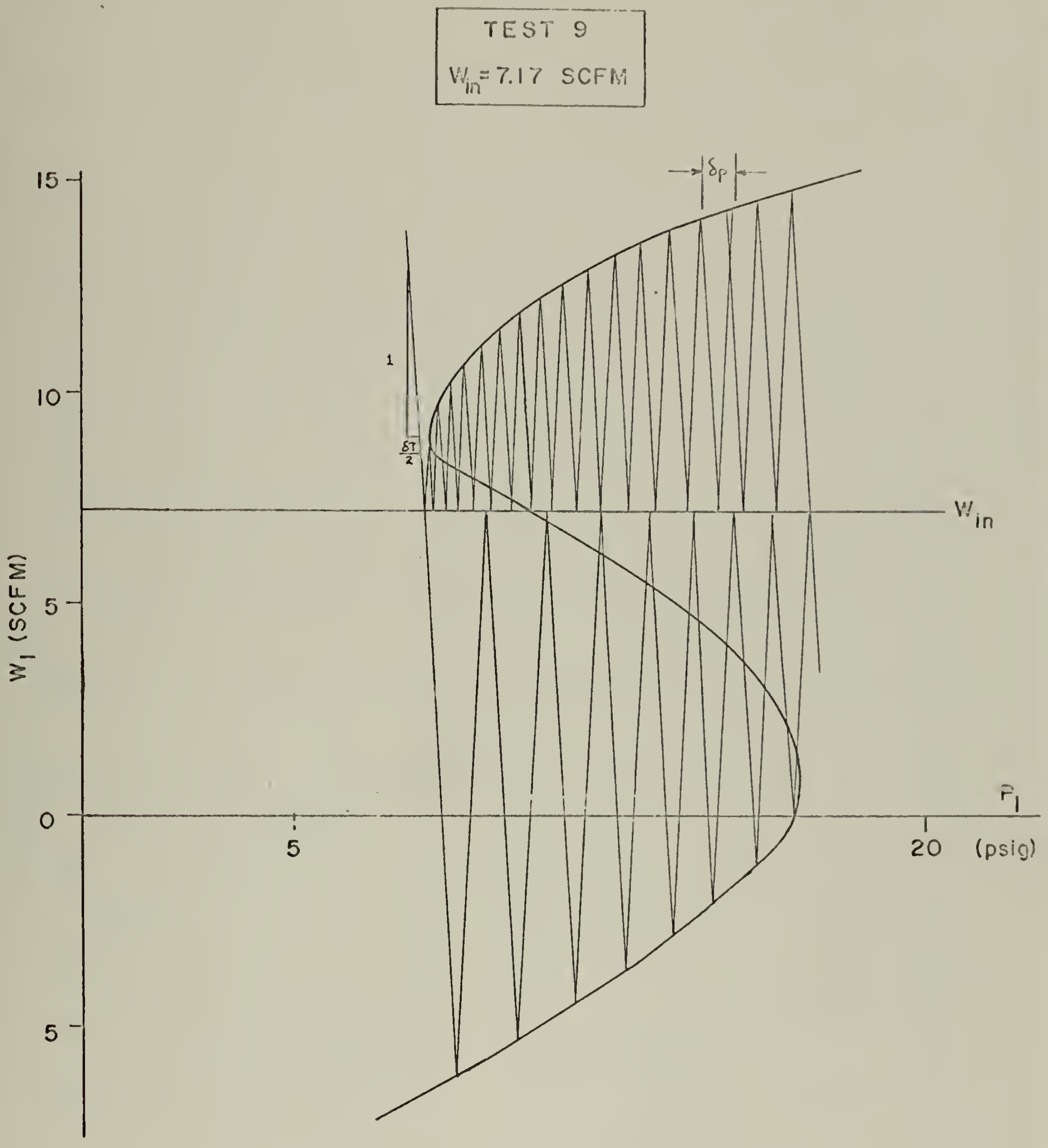

FIGURE 3.10 SLOPE LINE INTEGRATION TECHNIQUE

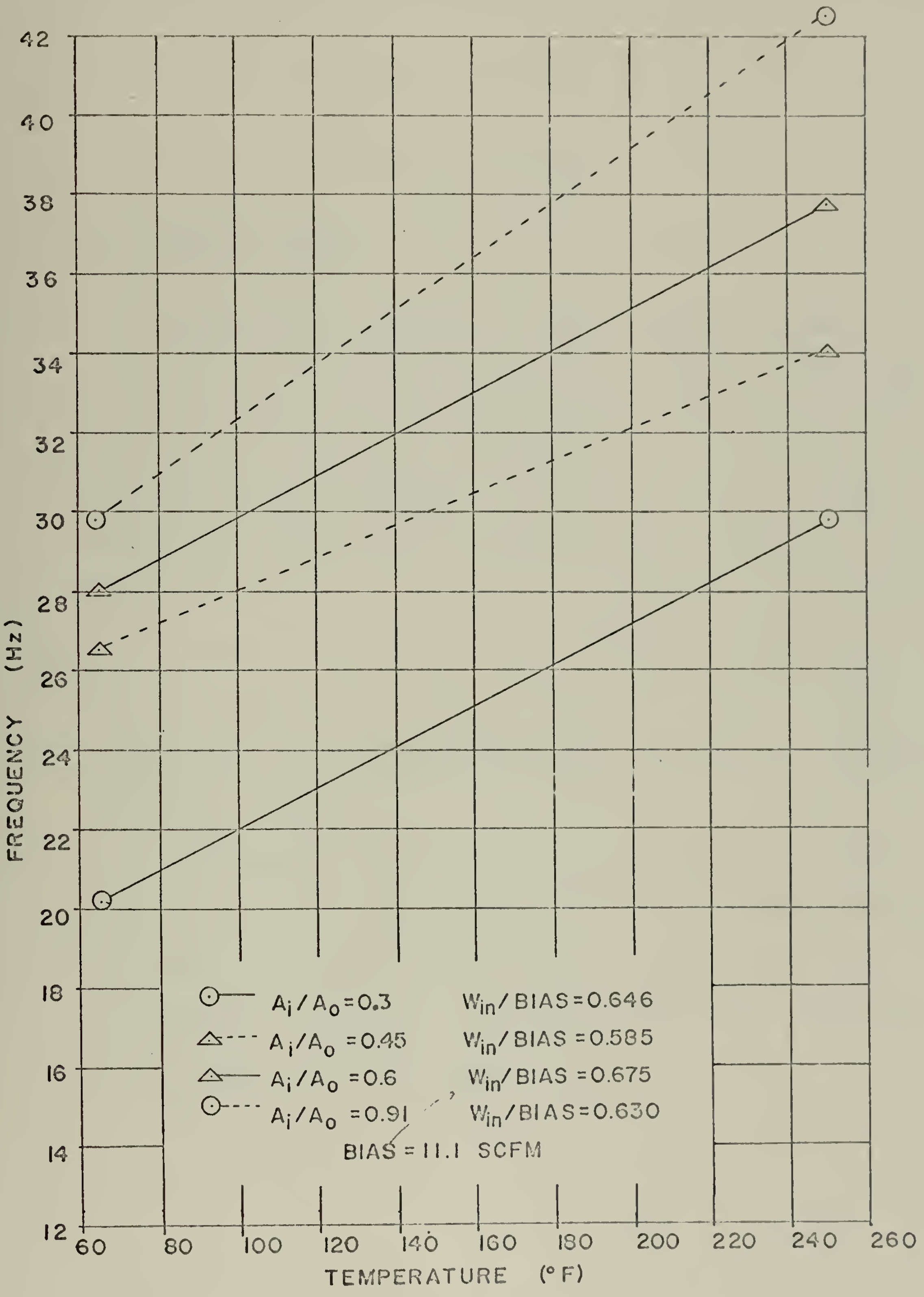

FIGURE 3.11 PREDICTED TEMPERATURE SENSITIVITY

CHAPTER IV

EXPERIMENTAL RESULTS

4.1 Geometric Effects

The geometry of the valve has many effects on its static characteristics. The static characteristic changes considerably as the inlet to outlet area ratio increases. The characteristic also changes with temperature. As the characteristic changes, so does the frequency and the output waveform. See Figures 4.1 and 4.2. Furthermore, the temperature sensitivity of the device can be changed by changing valve geometry as shown in Figure 3.10. The geometric configuration where $A_i/A_o = 0.60$ predicts a 34.6 percent change in frequency for a 35.2 percent change in absolute temperature.

The position of the inlet slots around the vortex chamber were varied holding A_i/A_o constant. It was found that spacing the inlets symmetrically or assymmetrically had little effect on the valve characteristic, provided the two sets of tangential inlets remained axially opposed.

The frequency of oscillation should be inversely proportional to the volume for a given vortex cavity geometry. Scaling down of the entire device should increase frequency if the laws of dynamic similitude apply. However, it is not clear how scaling down the vortex cavity effects the static characteristic of the device.

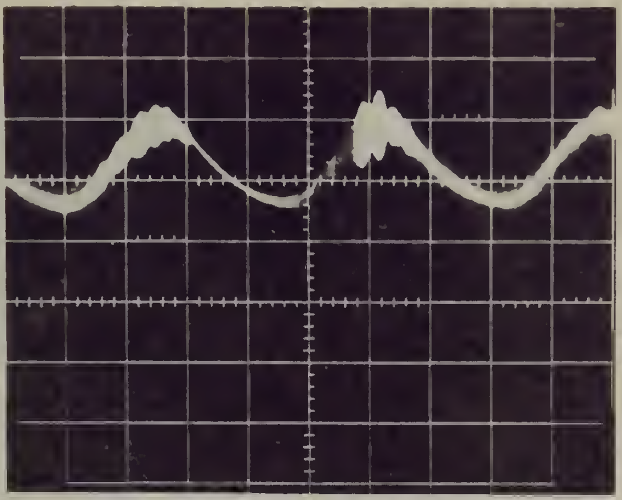

A_i/A_o = 0.30

W_{in}/ BIAS = 0.646

6.9 - 13.4 PSIG

TIME = 20 msec/cm

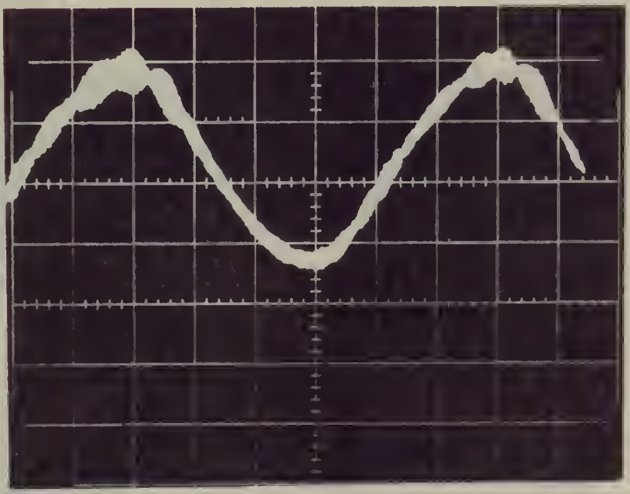

A_i/A_o = 0.45

W_{in}/ BIAS = 0.585

4.3 - 9.8 PSIG

TIME = 10 msec/cm

FIGURE 4.1 VOLUME PRESSURE HISTORY

[illegible]

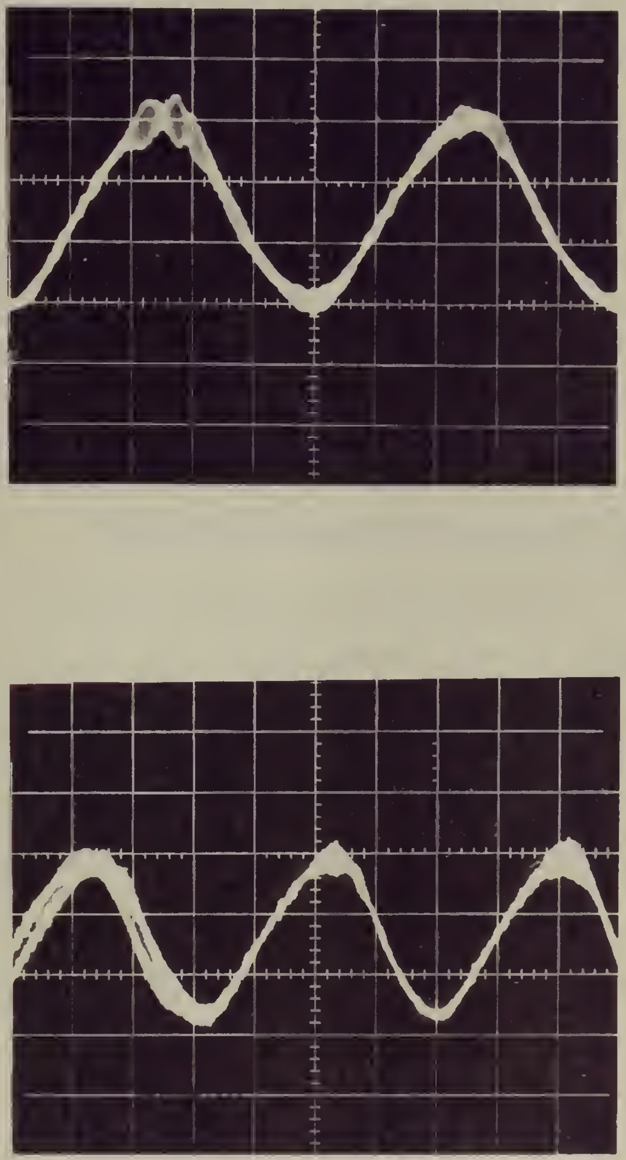

$A_i / A_o = 0.60$

$W_{in} / \text{BIAS} = 0.675$

3.3 - 8.1 PSIG

TIME = 10 msec/cm

$A_i / A_o = 0.91$

$W_{in} / \text{BIAS} = 0.630$

2.1 6.2 PSIG

TIME = 10 msec/cm

FIGURE 4.2 VOLUME PRESSURE HISTORY

4.2 Pressure Sensitivity

The device is very nearly insensitive to supply pressure if air temperature remains constant. The actual pressure sensitivity of the device is shown in Figure 4.3. The sensitivity was measured by setting flow conditions at a metering pressure of 40 psig. Supply pressure was then increased to 80 psig, then decreased to 10 psig. The ratio of flow into the volume to the bias flow remained nearly constant throughout the range tested.

4.3 Temperature Sensitivity

The ratio of predicted temperature sensitivity to actual temperature sensitivity was 3.2 to 1 for a given geometry. The main problem encountered while attempting to measure temperature sensitivity was a controllable constant temperature source. The fact that such apparatus was not available made it impossible to obtain steady state temperature data. A further shortcoming of the apparatus was that the device was constructed of brass and, therefore, provided a large heat sink.

However, temperature sensitivity data was obtained while the air temperature was steadily increasing. Though this is highly undesirable, it was the best information capable of being produced from this apparatus. To guard against misrepresenting the temperature sensitivity; temperature was measured at the valve inlet,

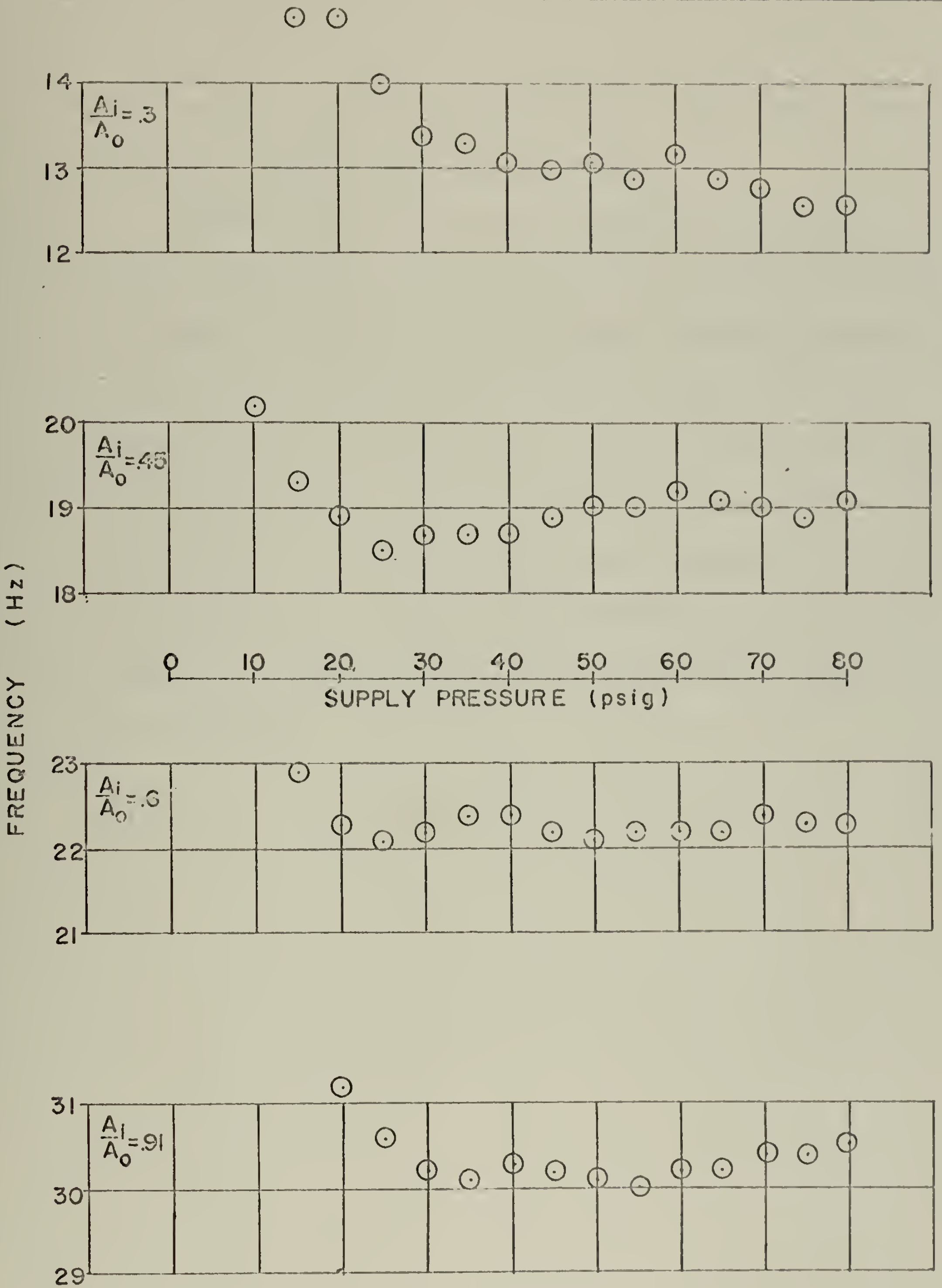

FIGURE 4.3 PRESSURE SENSITIVITY

valve outlet, and in the large volume. Table 4.1 clearly shows the large temperature gradients present.

Figure 4.4 shows the actual temperature sensitivity of the device, where temperature of the air in the volume is plotted. Although the sensitivity does not agree with that predicted in Section 3.4, the author feels that the undesirable thermal characteristics of the valve are a major cause of deviation. The predicted gain was obtained with the entire device at either 65° F or 250° F. However, steady state temperatures were not obtained during the temperature sensitivity tests. Further pursuit of temperature sensitivity data with this apparatus was not attempted.

TABLE 4.1

AIR TEMPERATURES

Inlet Temp (°F)	Outlet Temp (°F)	Volume Temp (°F)
65	65	65
80	77	70
97	92	80
116	106	90
126	117	100
139	127	110
152	140	120
162	150	130
171	159	140
181	170	150
191	181	160
200	190	170
210	201	180
219	211	190
226	220	200
235	229	210
245	240	220
253	251	230
262	262	240
270	270	250

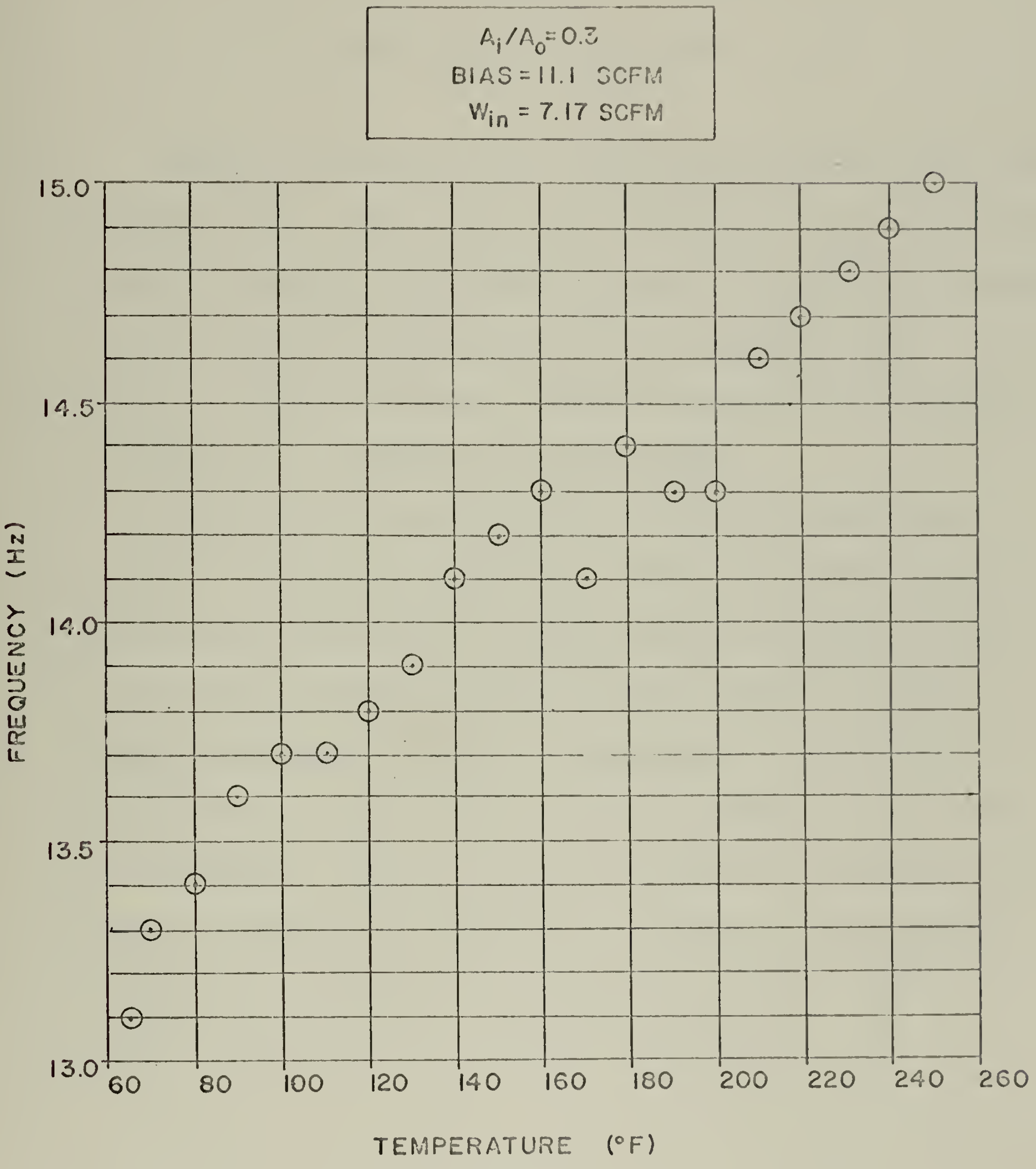

FIGURE 4.4 TEMPERATURE SENSITIVITY

CHAPTER V

CONCLUSIONS AND SUGGESTIONS

Geometric parameters have a significant influence on the valve characteristics. Herein lies an area where much more investigation should be conducted. The effect of each of the geometric parameters should be studied to lead eventually to an optimum design. The effect of scaling the device is vitally important to its eventual application and, therefore, should be studied.

This work has shown the device to be in fact temperature sensitive and pressure insensitive. Future work should begin by constructing a mold from the existing device and casting a new valve using a non-heat-conducting material, possibly plaster. Prior to attempting to measure the temperature sensitivity, a controllable temperature source must be obtained. If the results are acceptable, a device should be constructed of a material which follow the guidelines established in Appendix A. If a desirable temperature sensitive device is designed, it must be tested for speed of response to step changes in temperature.

APPENDIX

APPENDIX A

HEAT TRANSFER EFFECTS

To be a useful temperature sensor, it is desirable to sense the temperature of the air entering the device. The following is an order of magnitude study to determine a material which results in the least heat transfer to the device.

For this study, assume a solid homogenous body whose physical properties are constant; it is initially at a uniform temperature T_i, and is suddenly plunged into a fluid whose temperature is uniform at T_f; the heat transfer coefficient at the surface of the body remains constant.

Assume that the Biot number $(^k/hr_o)$ is greater than 6. With this assumption, the internal temperature gradients are negligible, i. e. the plate is thin.

An energy balance may be written for the body:

$$\text{Heat input} = \text{increase of internal energy}$$

$$dQ = Ah\,(T_f - T)\,dt = c\rho V\,dT \qquad (A.1)$$

With the assumptions made, integration of (A.1) yields:

$$t = \frac{c\rho V}{hA} \ln \frac{T_f - T_1}{T_f - T_2} \qquad (A.2)$$

Equation (A.2) gives the time required to heat the body from temperature T_1 to T_2.

Solving equation (A.2) for the time to rise 63.2 percent of the way between an initial and final temperature yields the time constant:

$$t = \frac{\rho c V}{hA} \qquad (A.3)$$

For the temperature sensor, we want the material to respond to a change in temperature quickly.

For flowing gases, the order of magnitude for h is 2 -50. The actual value will depend on the gas. The time constant decreases when the device is scaled down since V/A decreases with scaling. The best material to use to construct the device will have the smallest ρc product with the constraint that the Biot number is greater than 6. Table A.1 shows the thermophysical properties at 1112° F. The half thickness, r_o, of the material for this type device is on the order of 0.02 ft. Assuming h to be 50, the thermal conductivity, k, for a Biot number equal to 6 is on the order of 6. The ρc product for the various alloys listed in Table A.1 are the same order of magnitude.

The design of an operational device could isolate the device from its environment by constructing a plenum chamber around the entire device and discharge the exhaust gas from the valve into the plenum. This design should greatly reduce temperature gradients in the device.

TABLE A.1

THERMOPHYSICAL PROPERTIES AT 1112° F

	ρc (BTU/ft.^{3} °F)	k (BTU/hr.ft.°F)
Copper, pure	51.1	204
Iron, pure	53.3	23
Molybdenum	38.2	61
Nickel	59.0	32
Steel, mild	55.0	19
Stainless steel	53.5	13
Tungsten	38.6	65

The author feels a device constructed of stainless steel (k = 13) and designed to be isolated from its environment should minimize heat transfer to the device and thereby permit the device to be used as a sensor of input air temperature.

APPENDIX B

SLOPE-LINE INTEGRATION

This appendix describes slope-line integration in general and explains its use in analyzing the static valve characteristics. Reference (6) is the source of the general description of the technique.

See Figure B. 1. Suppose we are given two rectangles, A_1 and A_2, having equal bases Δx. The areas of the rectangles are therefore proportional to their heights, h_1 and h_2.

$$\frac{A_1}{A_2} = \frac{h_1}{h_2} \tag{B.1}$$

Suppose we are also given two inverted isosceles triangles each having the same vertex angle. The bases, a_1 and a_2, of the inverted isosceles triangles are also proportional to their heights, h_1 and h_2.

$$\frac{a_1}{a_2} = \frac{h_1}{h_2} \tag{B.2}$$

Therefore, the bases of the inverted isosceles triangles are proportional to the areas of the corresponding rectangles A_1 and A_2.

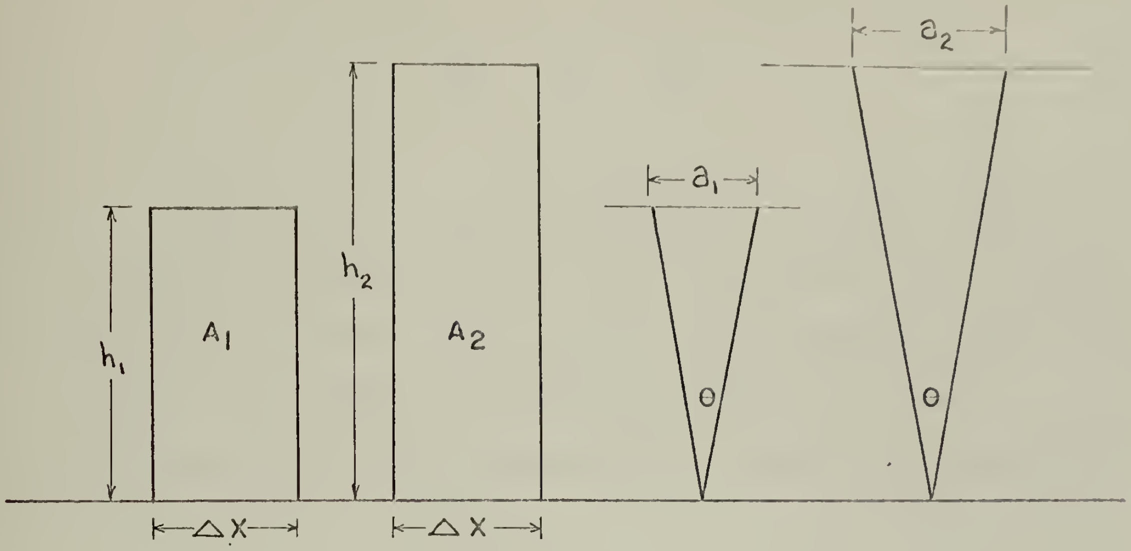

FIGURE B.1

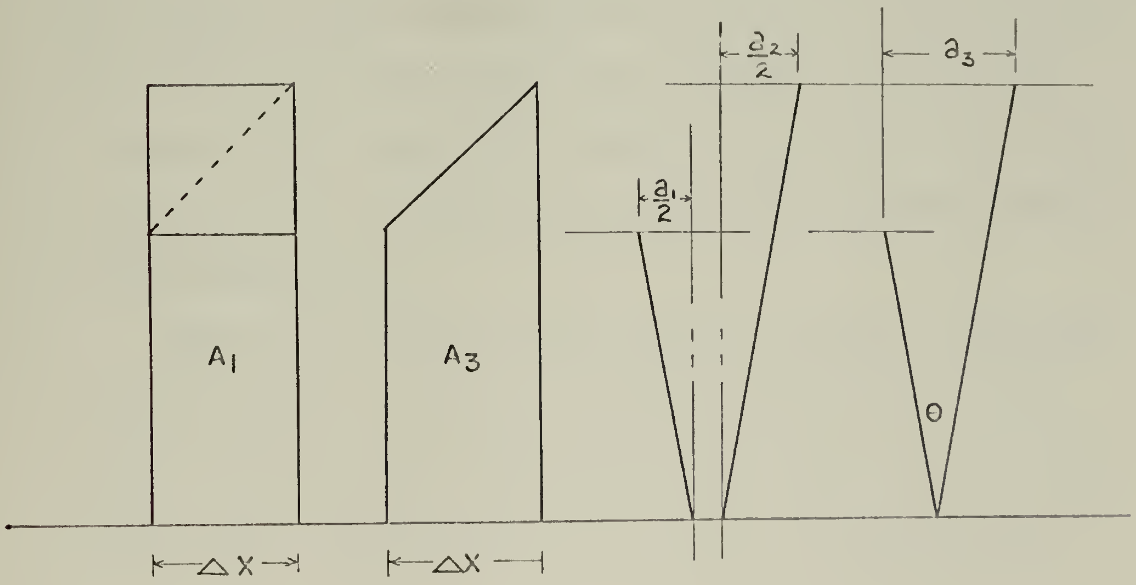

FIGURE B.2

$$\frac{A_1}{A_2} = \frac{h_1}{h_2} = \frac{a_1}{a_2} \qquad (B.3)$$

Suppose A_1 and A_2 were superimposed as shown in Figure B.2. They are in effect inscribed in and circumscribed about a trapezoid A_3. The area of $A_3 = 0.5\ (h_1 + h_2)\Delta x$ which is equal to the average area of the two rectangles A_1 and A_2; $A_3 = 0.5\ (A_1 + A_2)$. The area A_3 can be found graphically; therefore, by adding half of the "V" used to determine A_1 to half of the "V" used to determine A_2. The result is a "V" with a linear distance a_3 which is a measure of area A_3. See Figure B.2.

A curve can be approximated by a series of trapezoids; therefore, the area under the curve can be found graphically. If the widths of the trapezoids are all the same, a series of V's all having equal vertex angles will determine the area of the trapezoids. See Figure B.3. Note that the points in the slope-line diagram record the growth of area plotted against values of y, not values of x.

Suppose we assume that the procedure is exact. The assumption is valid if the curve is a polygon rather than a smooth curve. The procedure is more precise for a smooth curve as the width of the trapezoids approaches zero, i. e. steep slopes.

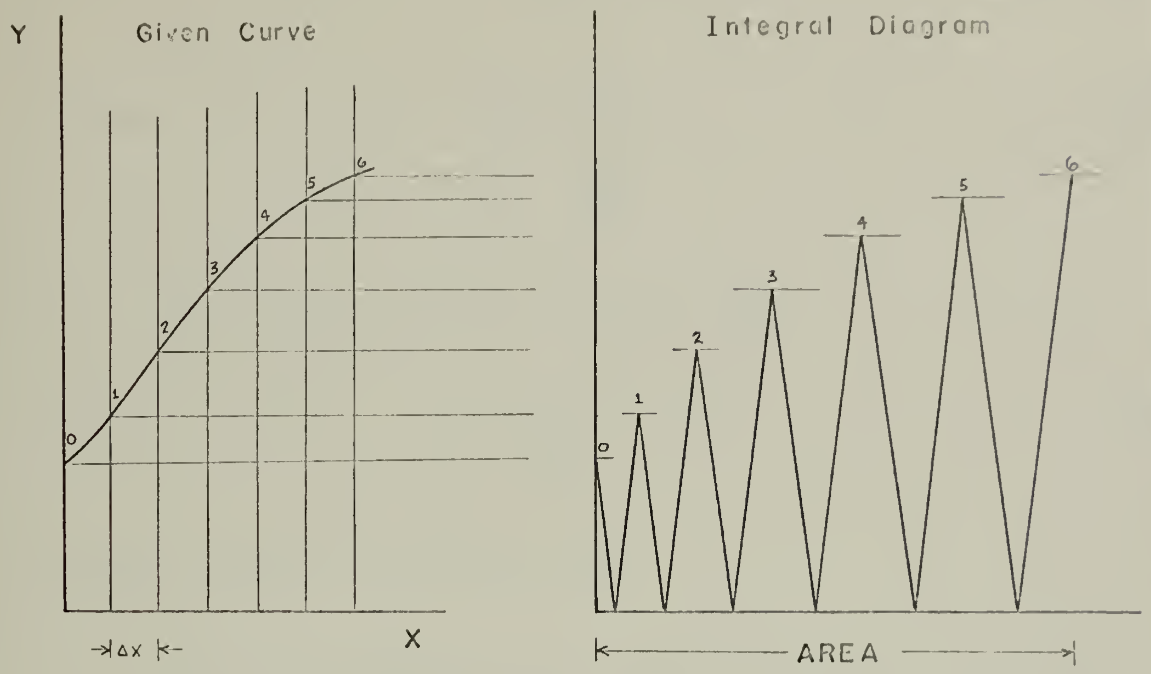

FIGURE B.3

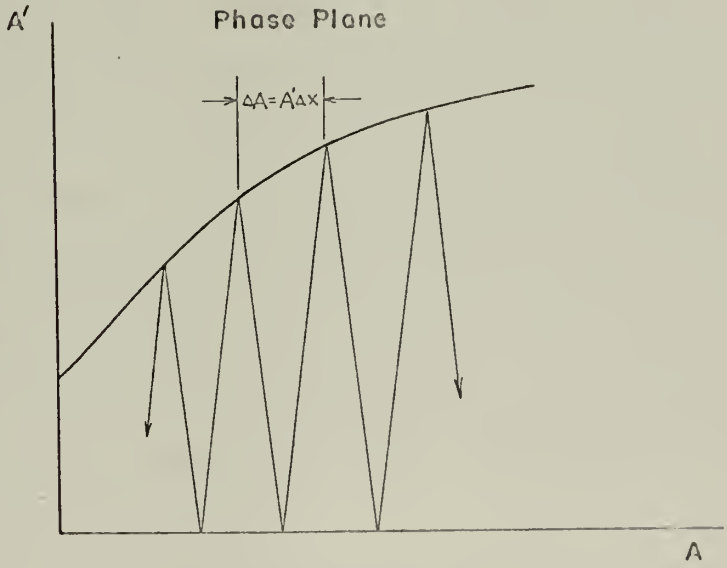

FIGURE B.4

Since
$$dA = ydx \qquad (B.4)$$

$$y = \frac{dA}{dx} \qquad (B.5)$$

Therefore, Figure B.3 can be viewed as:

$$A' = \frac{dA}{dx} = f(A) \qquad (B.6)$$

Such a graph is a phase-plane plot.

Now, let us suppose we were given a graph of A' as a function of A and we wish to obtain A as a function of x. We first choose a Δx interval. We then can set up the two slope-lines that constitute the V. In Figure B.4 we see that $\Delta A = A' \Delta x$ since the area of a rectangle $A' \Delta x$ can be represented by ΔA. We now start at any point on the curve and construct the slope-lines from the given curve to the axis and back to the curve, etc. We obtain a series of points on the curve spaced Δx units apart. We can now calibrate these points with appropriate values of x. When we have finished, we can plot A as a function of x. We have successfully solved the differential equation (B.6). We can start anywhere along the curve since this reflects the arbitrary choice of the constant of integration.

The direct application to the analysis for the static valve characteristic is discussed in the following paragraphs. The analogy that can be drawn between the present analysis and the

previous discussion is straightforward. The static valve characteristics together with the flow into the volume, W_{in}, represent a phase-plane plot. Since the net flow rate into the volume, $W_{in} - W_1 = \tau \frac{dp}{dt}$ is plotted against p. Therefore, the analogous quantities are:

A	p
x	t
$\frac{dA}{dx}$	$\frac{dp}{dt}$

Since we are given a graph of $\frac{dp}{dt}$ as a function of p, we can plot p as a function of t and, therefore, can obtain the frequency of oscillation.

The procedure is to establish slope-lines of slope $\delta\tau/2$ as shown in Figure 3.10 and construct the zig zag pattern between W_{in} and W_1. The linear distance between the V's represent δp. We obtain a series of points on the curve spaced $\delta\tau$ units apart. We can now plot p as a function of τ and thus determine the period of oscillation. The period can be related to real time through the equation

$$\delta t = \frac{V}{kRT}\,\delta\tau$$

and thus the frequency of oscillation can be computed.

REFERENCES

1. "Basic Applied Research in Fluid Power Control", Report No. 6310-2, Dept. of Mech. Engr., Engineering Projects Laboratory, Mass. Inst. of Tech., Cambridge, Mass., January, 1967. AFFDL - TR - 60 - 723.

2. "Basic Applied Research in Fluid Power Control", Report No. 76310-1, Dept. of Mech. Engr., Engineering Projects Laboratory, Mass. Inst. of Tech., Cambridge, Mass., August, 1966. AFFDL - TR - 66 - 130.

3. "Basic Applied Research in Fluid Power Control", Report No. 5393-2, Dept. of Mech. Engr., Engineering Projects Laboratory, Mass. Inst. of Tech., Cambridge, Mass., July, 1965. AFFDL - TR - 65 - 130.

4. "Basic Applied Research in Fluid Power Control", Report No. 5393-1, Dept. of Mech. Engr., Engineering Projects Laboratory, Mass. Inst. of Tech., Cambridge, Mass., May, 1965. AFFDL - TR - 65 - 79.

5. Bell, A. C., "Optimization of a Vortex Valve". Thesis (S. M.), Dept. of Mech. Engr., Mass. Inst. of Tech., Cambridge, Mass., December, 1965.

6. Rule, J. T. and Coons, S. A., "Graphics", McGraw-Hill Book Company, Inc., New York, Toronto, and London, 1961.

7. Blackburn, J. F., Reethof, G. and Shearer, J. L., "Fluid Power Control", Technology Press of M. I. T. and John Wiley and Sons, Inc., New York and London, 1960.

8. Rohsenow, W. M. and Choi, H. Y., "Heat, Mass, and Momentum Transfer", Prentice-Hall, Inc., Englewood Cliffs, New Jersey, 1961.

thesP4868
Pneumatic oscillator using a vortex ampl
3 2768 001 92378 2
DUDLEY KNOX LIBRARY